ARTICLE

Terahertz emission from zinc oxide and low-temperature grown gallium arsenide photoconductive antennas: a comparative analysis using Drude-Lorentz and equivalent circuit models

Jose Mari Sebastian C. Arcilla*, Lourdes Nicole F. Dela Rosa, Vince Paul P. Juguilon, Ivan Cedrick M. Verona, Dhaniel Angelo Batalla, Alexander E. De Los Reyes, Hannah R. Bardolaza, and Elmer S. Estacio

National Institute of Physics, University of the Philippines-Diliman

ABSTRACT

The terahertz (THz) emission characteristics of zinc oxide (ZnO) and the widely used low-temperature-grown gallium arsenide (LT-GaAs) photoconductive antennas (PCA) were investigated and compared by employing the Drude-Lorentz model and the equivalent circuit model (ECM). The calculated peaks are 79.34 V/m, and 21.58 V/m for LT-GaAs, and ZnO, respectively using the Drude-Lorentz model. Meanwhile, via the ECM, the THz emission peak values are 2.34 V/m, and 1.59 V/m for LT-GaAs, and ZnO, respectively. Additionally, we also demonstrated the laser pump power (P_{pump}) dependence and bias voltage (V_{bias}) dependence of both substrates using the Drude-Lorentz model, and ECM, then subjected both substrates to their respective literature-reported breakdowns for breakdown voltage (V_B) and optical damage threshold (P_B). The maximum emission values until V_B were calculated to be 307.34 V/m for LT-GaAs, and 1292.48 V/m for ZnO using the Drude-Lorentz model. Subsequently for ECM, the maximum emission values before V_B were 14.05 V/m, and 95.11 V/m for LT-GaAs and ZnO respectively. Similarly, the maximum emitted THz values until P_B for the Drude-Lorentz model were 317.34 V/m for LT-GaAs, and 323.66 V/m for ZnO. On the other hand, using ECM, the

*Corresponding author
Email Address: jcarcilla@up.edu.ph
Date received: March 7, 2024
Date revised: July 19, 2024
Date accepted: July 19, 2024
DOI: https://doi.org/10.54645/2025181LIF-21

KEYWORDS

Semiconductor Physics, Drude-Lorentz model, Equivalent Circuit model, voltage breakdown, optical damage threshold

maximum emitted values before P_B were 210.87 V/m, and 327.90 V/m for LT-GaAs, and ZnO, respectively. These findings offer valuable insights for choosing the optimal parameters in the design and operation of future ZnO and LT-GaAs-based PCA material.

INTRODUCTION

The frequency range of the electromagnetic spectrum spanning from 100 gigahertz (GHz) to 10 terahertz (THz) is commonly referred to as the terahertz (THz) band (Lee 2009). In studying this frequency range, the commonly used optoelectronic device is the photoconductive antenna (PCA) since it allows for an efficient and effective way of studying the THz frequency range (Umezawa et al. 2009). The PCA is a semiconductor substrate that operates upon the application of a bias voltage (V_{bias}) and the subsequent optical excitation using a femtosecond laser, which emits photons that have photon energy greater than the band gap of the semiconductor material. This process effectively enables the PCA to emit THz radiation, given by

$$J = en(t)v(t) \tag{1}$$

where n(t) is the photocarrier density, v(t) is photocarrier velocity, and e is the elementary charge (Jepsen et al. 1996).

Experimental studies on the THz emission characteristics of PCAs can be costly and time-consuming, hence, theoretical models can be advantageous in performing parametric studies. One of the models under consideration in this work is the Drude-Lorentz model. It is the combination of both the Drude model, which describes the transport properties of electrons in metals, and the Lorentz model which incorporates the frequency response of dielectric materials. The combination of the two models provides a simple but effective method for explaining the photocarrier transport dynamics within the PCA.

Equation 1 can be solved using the given differential equation as stated by the Drude-Lorentz model,

$$\frac{dv(t)}{dt} = -\frac{v}{\tau_s} + \frac{e}{m^*}E_{loc} \tag{2}$$

$$\frac{dP_{sc}}{dt} = -\frac{P_{sc}}{\tau_r} + J(t) \tag{3}$$

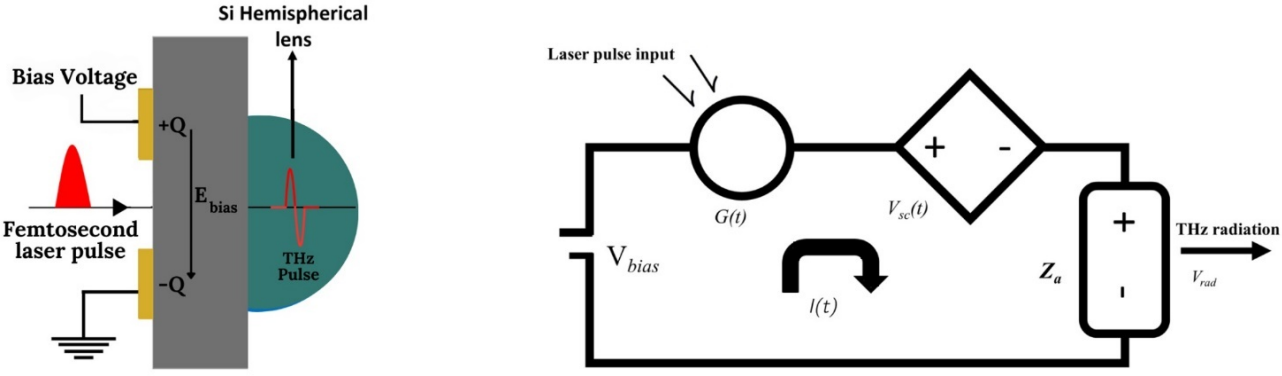

Figure 1: Schematic diagram of a PCA and its equivalent circuit model (ECM) using PCA as an emitter (Lee 2009; Loata et al. 2007).

From Kirchoff's loop rule, the continuity equation for the voltages is given by (Loata et al. 2007),

$$V_{bias} = V_{gap}(t) + V_{rad}(t) + V_{sc}(t). \tag{7}$$

Where $V_{rad}(t)$ is the voltage of the radiating element, and $V_{sc}(t)$ is the screening voltage due to space charge polarization.

$$\frac{dn(t)}{dt} = -\frac{n}{\tau_c} + g(t) \tag{4}$$

where $\boldsymbol{\tau}_s$ is the scattering time, m* is the electron's effective mass, E_{loc} is the electric field at the carriers' position, P_{sc} is the polarization due to carrier separation, $\boldsymbol{\tau}_r$ is the recombination time of photocarriers, g(t) is the laser generation rate term, and $\boldsymbol{\tau}_c$ is the material's carrier lifetime.

Meanwhile, the Equivalent Circuit Model (ECM) is another method employed in simulating the THz emission of PCA systems that are based on the Drude-Lorentz model. In this system, the PCA is able to be modelled by a circuit with time varying elements that is operating in the THz frequency range. As depicted in Fig. 1, the ECM represents the PCA as an emitter (Loata et al. 2007), and it is represented by three circuit elements that are in series with one another which are connected to a DC voltage source. The ECM employed by Loata et al. was selected for its simplicity and its ability to closely match the experimental data (Loata et al. 2007). Applying circuital laws on Fig. (1), the time varying voltage on the gap (V_{gap}) is expressed as (Loata et al. 2007; Khiabani et al. 2013)

$$\frac{dV_{gap}(t)}{dt} = \left[V_{bias} - V_{gap}(t)\left(\frac{1 + e\mu_e n(t)\tau_r}{\eta\mathcal{E}} + Z_a\tau_r\frac{dG(t)}{dt} + G(t)Z_a\right)\right] \times \left(\frac{1}{\tau_r(1 + G(t))Z_a}\right) \tag{5}$$

Where η is the screening factor, ε is the dielectric constant of the material, μ_e is carrier mobility of the material and the conductance (G(t)) is dependent on the carrier density (n(t)) given by Eq. 4 of the Drude-Lorentz model (Khiabani et al. 2013). The conductance is expressed as

$$G(t) = e\mu_e n(t)\frac{S}{l} \tag{6}$$

where, S is the active antenna area, and l is the antenna gap length.

In this work, the ECM and Drude-Lorentz models were utilized in simulating the THz emission of ZnO and LT-GaAs PCAs. From the obtained results, we compare the ZnO and LT-GaAs PCAs performances. The results acquired from the two different models will allow us to identify the strengths and limitations of both models, as well as to verify consistency in trends.

METHODOLOGY

In simulating the THz generation using the Drude-Lorentz model we used Python v.3.8.10. Equations (2), (3), and (4) were solved via the ODEINT function from the SciPy library. From these equations, we acquire the values of n(t) and v(t), and subsequently compute for J(t). We solved for the time derivative of J(t) to be able to calculate the emitted THz radiation. We note that the emitted THz radiation in the simulation is approximated by a Hertzian dipole expressed as,

.

$$E_{THz} = \frac{\mu_0 A}{4\pi z}\frac{dJ_s(t_r)}{dt} \quad (8)$$

where μ_0 is the permeability of free space, A is the optically excited area, and $J_s(t_r)$ is the surface current density (Lee 2009). We can observe in Eq. (8) that the emitted THz signal is proportional to the time derivative of the current density ($E_{THz} \propto \frac{dJ_s(t_r)}{dt}$).

Similarly, the ECM simulation was done via Python v.3.8.10. Equation (5) was solved through SciPy ODEINT which resulted in the voltage at gap (V_{gap}). The V_{sc} is obtained from solving the time derivative of the $P_{sc}(t)$ in Eq. 3

The voltage of the radiating element (V_{rad}) is then expressed as (Khiabani et al. 2013)

$$V_{rad}(t) = Z_a en(t)\mu_e V_{gap}\frac{S}{l} \quad (9)$$

which is characterized by the impedance, Za (which is assumed to be purely resistive, and independent of frequency over the significant THz frequencies).

We would then compute for the current density of the radiating element (j(t)) expressed as

$$j(t) = en(t)\mu_e V_{gap}(t)\frac{S}{l} \quad (10)$$

by taking the time derivative of Eq. (10) we get the value of the emitted THz radiation of the ECM.

Listed in Table 1 are the electrical, physical, and optical constants used in the simulation as well as the literature obtained material parameters for both ZnO and LT-GaAs (Ozgur et al. 2005; Acharya et al. 2004; Vegesn et al. 2020; Aguilar et al. 2019; Norton et al. 2004; Khiabani et al. 2013).

Table 1: List of parameters used from available literature values

		ZnO		LT-GaAs		
Parameter	Notation	Drude	ECM	Drude	ECM	Unit
Laser Wavelength	λ	290	290	780	780	nm
Electron Mobility	μ_e	210	210	150	150	cm^2/Vs
Electron effective mass	m*	0.24	0.24	0.067	0.067	-
Dielectric constant	κ	9.34	9.34	13	13	-
Reflection Coefficient	R	0.1	0.1	0.318	0.318	-
Optical Absorption	α	8.22×10^4	8.22×10^4	12.0×10^5	12.0×10^5	cm^{-1}
Depth of excitation region	d_0	1.00×10^{-6}	1.00×10^{-6}	1.00×10^{-6}	1.00×10^{-6}	-
Carrier Lifetime	τ_c	2	2	3	3	ps
Carrier Recombination	τ_r	110	110	100	100	ps
Screening factor	η	900	900	900	900	-
PCA Gap length	l	5	5	5	5	μm
PCA gap width	w	10	10	10	10	μm
Applied bias voltage	V_{bias}	10	10	10	10	V
Laser pump power	P_{pump}	10	10	10	10	mW
Antenna resistance	Z_a	-	60	-	130	**Ω**

RESULTS AND DICUSSIONS

Figure 2(a) illustrates the comparison of the THz emission from LT-GaAs and ZnO using the ECM and Drude-Lorentz model. We observe from Fig. 2(a) that the peaks obtained using the Drude-Lorentz model are 79.34 V/m, and 21.58 V/m for LT-GaAs, and ZnO, respectively. Similarly, the calculated THz peaks from ECM for LT-GaAs, and ZnO are 2.34 V/m, and 1.59 V/m, respectively. We can observe from these values that generally, THz emissions for both PCAs via the Drude-Lorentz model are much greater than the results via the ECM. This difference in emission values can be attributed to the fact that the ECM has taken into account two screenings, namely the space charge screening, and the radiation field screening. On the other hand, the Drude-Lorentz model only considers the space charge screening.

Seen in Fig. 2(b) is the FFT spectra of both the Drude-Lorentz and ECM. The bandwidth indicates the velocity distribution of accelerated photocarriers. The bandwidth for both the Drude-Lorentz model and ECM are ~9 THz, and ~4 THz for LT-GaAs, and ZnO, respectively. We note that the models used in the simulation did not account for the generation of longitudinal optical (LO) phonons, which are generated due to the voltage biasing, and laser pumping of the semiconductor substrate effectively increasing the lattice structure of both substrates (Wu et al. 2019). These phonons are generated and absorbed at

specific frequencies by both semiconductor substrates, this then leads to the termination of emission (Dekorsy et al. 1993).

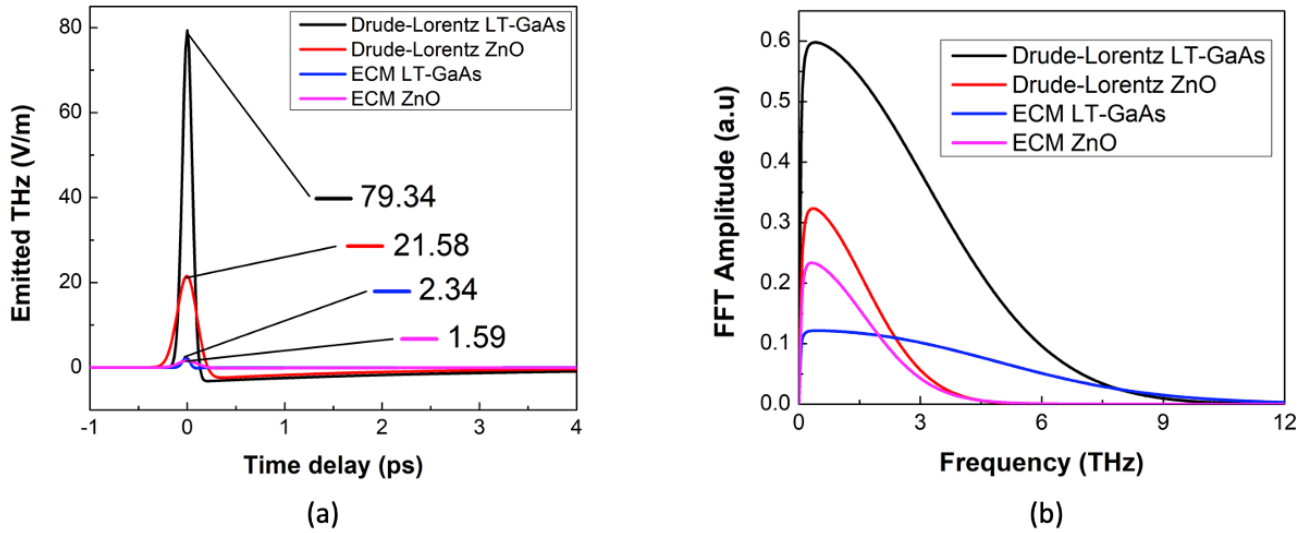

Figure 2: Emitted terahertz of LT-GaAs and ZnO through ECM and Drude-Lorentz (a) along with their respective FFT spectra (b)

Figure 3 demonstrates the voltage and laser power dependence using the Drude-Lorentz model, and ECM until the literature reported values of voltage breakdown (V_B) and optical damage threshold (P_B). It is important to note that at values greater than V_B and P_B the substrates would have already sustained damage allowing no further emission of THz radiation. In simulating the parameter dependence of both substrates through both models, all listed parameters in Table 1 were held constant while the chosen parameter was varied to different values. It should be pointed out, that LT-GaAs projected value disregards the damage threshold of LT-GaAs, and it is under the assumption that no breakdown or damage occurs. The literature reported V_B of LT-GaAs, and ZnO are 60 V, and 599 V, respectively (Ma et al., 2019; Xie et al. 2019). The emission values of each substrate before their respective V_B are computed to be 307.34 V/m for LT-GaAs, and 1292.48 V/m for ZnO using the Drude-Lorentz model. Similarly, for ECM the emission values before V_B are calculated to be 14.05 V/m, and 95.11 V/m for LT-GaAs, and ZnO respectively.

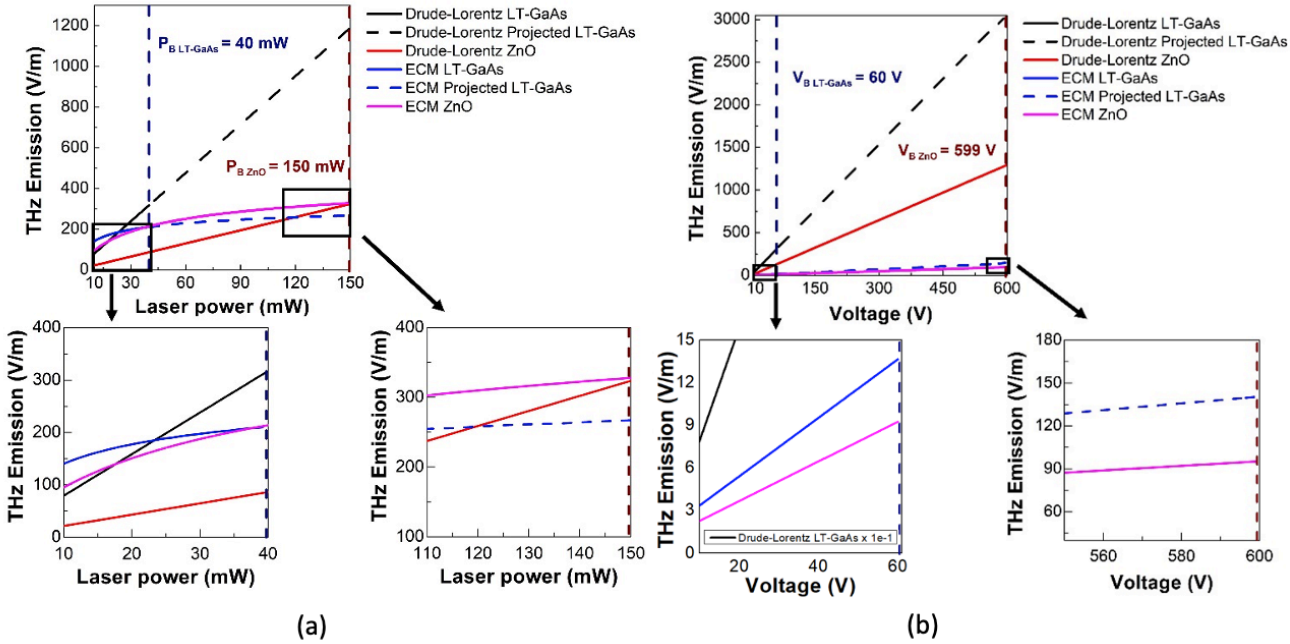

Figure 3: Laser power dependence (a) and Voltage dependence (b) of LT-GaAs and ZnO through ECM and Drude-Lorentz

Additionally, emission values before the P_B are also investigated. The documented optical damage threshold for LT-GaAs is 40 mW, and 150 mW for ZnO (Hong et al. 2013). The peak emission values of LT-GaAs, and ZnO before P_B are calculated to be 317.34 V/m, and 323.66 V/m respectively, using the Drude-Lorentz model. For ECM the peak emission values before P_B are computed to be 210.87 V/m for LT-GaAs, and 327.90 V/m for ZnO. Seen in Fig. 3(b) that the values of ECM saturate when compared to the values of the Drude-Lorentz model. This is due to additional screening of the ECM, that is the radiation field screening of the local electric field that is caused by PCA under ECM are excited by high repetition femtosecond lasers (Loata et al. 2007). It is also evident from the graph the the saturation level of LT-GaAs is lower as compared to ZnO. This is attributed to the radiation field screening attenuating the emitted THz; therefore, stronger THz sources would approach a saturation level earlier.

We observe that the LT-GaAs THz emission displays increased intensity at lower values of V_{bias} and P_{pump}. However, as we

incrementally increase the values of V_{bias} and P_{pump} to each substrate's respective V_B and P_B, the ZnO PCA produces a relatively more intense THz emission, attributed to its higher voltage and optical threshold breakdowns which is evident in both models.

We generally see that ZnO has more efficient THz emission characteristics than LT-GaAs at breakdown with respect to their THz emission intensity. This is attributed to the fact that ZnO is a wide band gap semiconductor. As a result, it can withstand high electric fields and operate at high temperatures (Tien and Ho 2019). Zinc oxide's high heat capacity, melting point, and conductivity and minimal thermal expansion are advantageous characteristics of ZnO that allow it to operate at high power conditions (Moezzi et al. 2012; Porter 1991).

CONCLUSION

We were able to simulate the THz emission from both Drude-Lorentz and Equivalent Circuit models. The computed peaks of LT-GaAs and ZnO using the Drude-Lorentz model are 79.34 V/m, and 21.58 V/m respectively. Similarly for ECM, we calculated 2.34 V/m for LT-GaAs and 1.59 V/m for ZnO. We have also shown a parametric study regarding the voltage dependence and laser power dependence from both models where we evaluated each substrate using both models independently to their respective V_B and P_B. The voltage dependence shows that the maximum emission values of LT-GaAs, and ZnO are 307.34 V/m, and 1292.48 V/m, respectively using the Drude-Lorentz model. Meanwhile for ECM, the emission values until V_B are 14.05 V/m for LT-GaAs and 95.11 V/m ZnO. Furthermore, investigating laser power dependence for both substrates showed that, using the Drude-Lorentz model, LT-GaAs reached maximum emission values of 317.34 V/m, and ZnO reached 323.66 V/m. In contrast, the ECM produced values of 210.87 V/m, and 327.90 V/m for LT-GaAs and ZnO respectively. Results show that LT-GaAs exhibit better THz emission at low power values of V_{bias} and P_{pump}, but at high power values of V_{bias} and P_{pump} ZnO showcases a more efficient THz emission. These findings contribute to determining the optimized parameters of PCA for future PCA THz-Time Domain Spectroscopy studies. They also demonstrate that while the Drude-Lorentz model fails to account for saturation effects at large parameter values, the ECM effectively captures these saturation levels. Thus, it is also important to choose which model is applicable for semiconductor substrates with low and wide band gap.

ACKNOWLEDGMENT

This work was supported in part by the Department of Science and Technology - Philippine Council for Industry, Energy, and Emerging Technology Research and Development - Grants in Aid (DOST-PCIEERD GIA Project No. 11336.).

CONFLICT OF INTEREST

The authors declare that there is no conflict of interest.

CONTRIBUTIONS OF INDIVIDUAL AUTHORS

Arcilla developed the Python code, compiled relevant literature, and conducted the necessary simulations, as well as wrote the manuscript. Dela Rosa, Verona, and Juiguilon provided guidance in optimizing the Python code and offered valuable insights for writing the R&D section. Batalla performed partial simulations related to the ECM results. De los Reyes, Bardolaza, and Estacio provided critical feedback and revisions for the manuscript. All authors approved the final version of the manuscript prior to submission.

REFERENCES

Lee YS. Generation and Detection of Broadband Terahertz Pulses. ed. Principles of terahertz science and technology. San Francisco: Springer, 2009.

Acharya S, Chouthe S, Graenez H, Böntgen T, Sturm C, Schmidt-Grund R, Grundmann M, Seifert G. Ultrafast dynamics of the dielectric functions of ZnO and BaTiO3 thin films after intense femtosecond laser excitation. J. Appl. Phys. 2014; 115(5): 053508.

Aguilar O, de Castro S, Godoy MPF., Dias MR.S. Optoelectronic characterization of Zn1-xCdxO thin films as an alternative to photonic crystals in organic solar cells. Opt. Mater. Express 2019; 9(9): 3638-3648

Castañeda-Uribe OA, Criollo CA., Winnerl S, Helm M, Avila A. Comparative study of equivalent circuit models for photoconductive antennas. Opt. Express 2018; 26(22): 29017-29031.

Hong S, Yeo J, Manorotkul W, Kim G, Kwon J, An K, Ko SH. Low-temperature rapid fabrication of zno nanowire uv sensor array by laser-induced local hydrothermal growth. J. Nanomater 2013; 2013(1): 246328.

Khiabani N, Huang Y, Shen YC, Boyes S. Theoretical modeling of a photoconductive antenna in a terahertz pulsed system. IEEE Trans. Antennas Propag 2013; 61(4):1538-1546.

Loata G, Thomson MD, Löffler T, Roskos HG. Radiation field screening in photoconductive antennae studied via pulsed terahertz emission spectroscopy. Appl. Phys. Lett. 2007; 91(23):232506.

Ma C, Yang L, Dong C, Wang S, Shi W, Cao J. An experimental study on lt-gaas photoconductive antenna breakdown mechanism. IEEE Trans. Electron Devices. 2018; 65(3):1043-1047.

Moezzi A, McDonagh AM, Cortie MB. Zinc oxide particles: synthesis, properties and applications. Chem. Eng. J. 2012; 185-186:1-22.

Norton D, Heo Y, Ivill M, Ip K, Pearton S, Chisholm M, Steiner T. ZnO: growth, doping and processing. Mater. Today 2004; 7(6):34-40.

Özgür Ü, Alivov YI, Liu C, Teke A, Reshchikov M, Doğan S, Avrutin VC, Cho SJ, Morkoç AH. A comprehensive review of ZnO materials and devices. J. Appl. Phys. 2005; 98(4):041301.

Porter F. PROPERTIES. In: Faulkner LL., ed. Zinc handbook: properties, processing, and use in design. 1st edition. Boca Raton: CRC Press, 199:36-57.

Tien, LC, Ho CH. Synthesis, optical characterization, and environmental applications of β-Ga2O3 nanowires.In: Pearton S, ed. Gallium Oxide. Elsevier, 2019:67-90.

Uhd Jepsen P, Jacobsen RH, Keiding SR. Generation and detection of terahertz pulses from biased semiconductor antennas. J Opt Soc Am 1996; 13(11): 2424-2436.

Umezawa R, Nagasaka R, Cadatal M, Ono S, Sarukura N Ichikawa Y. Terahertz-Radiation photoconductive antenna in sputtered zinc oxide thin film. Jpn. J. Appl. Phys. 2009; 48(3):030209.

Vegesn SV, Bhat VJ, Bürger D, Dellith J, Skorupa I, Schmidt OG, Schmidt H. Increased static dielectric constant in ZnMnO and ZnCoO thin films with bound magnetic polarons. Sci.; 10(1).

Xie G, Wu M, Shi W. Boundary breakdown time of ZnO varistors under nanosecond pulse current. AIP Advances 2019; 9(4):045032.

Wu, Y, Chen Z, Nan P, Xiong F, Lin S, Zhang X, Chen Y, Chen L, Ge, Pei Y, Lattice strain advances thermoelectrics. Joule 2019; 3(5): 1276-1288

Dekorsy T, Kurz H, Zhou XQ, Ploog K, Investigation of field carrier and coherent phonon dynamics in low-temperature grown gaas. Appl. Phys. Lett. 1993; 63(21): 2899–2901.